SUPPLEMENTARY DATA

Table of Contents

Supplementary Figure S1

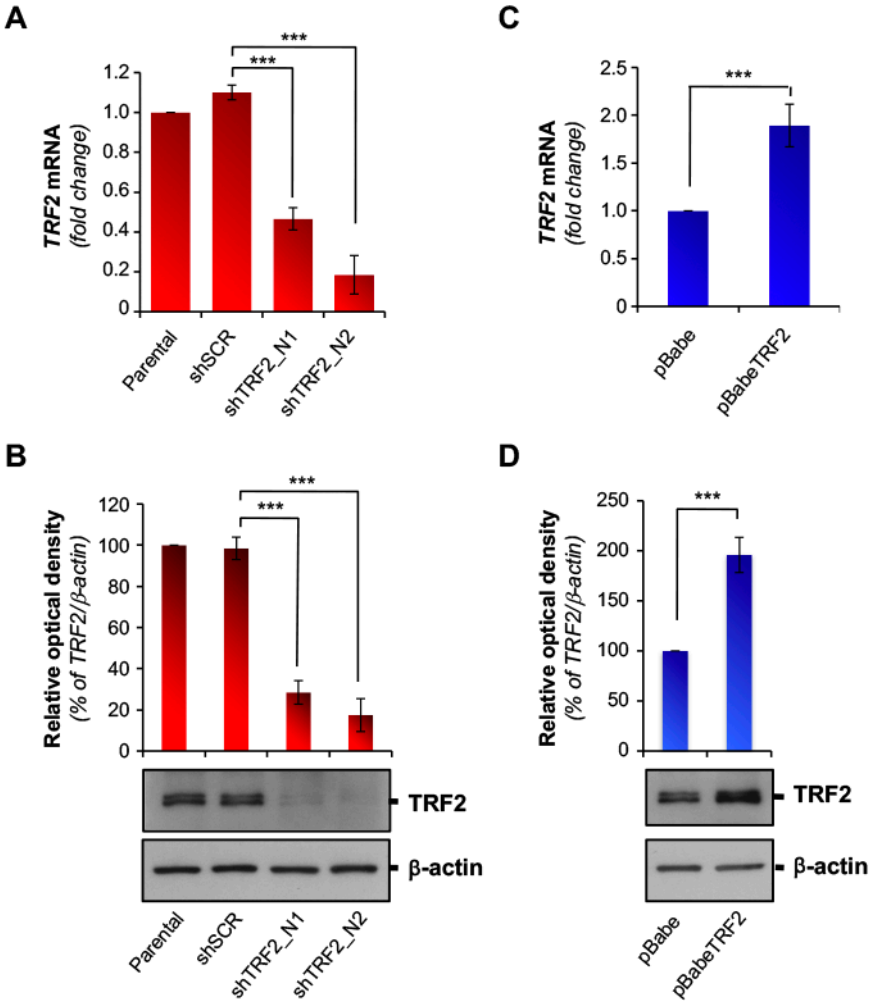

Supplementary Figure S1: Modulation of TRF2 expression levels in HCT116 cells.
Levels of TRF2 expression were evaluated in stable HCT116 cell lines **(A and B)** silenced (shTRF2_N1 and shTRF2_N2) or **(C and D)** overexpressing (pBabe-TRF2) TRF2 and in their control counterparts (shScramble/ pBabe) and, where indicated, in uninfected (parental) cells. **(A and C)** Quantitative evaluation of gene expression by *real-time* RT-PCR. Results are expressed as fold change of mRNA levels in silenced **(A)** or overexpressing **(C)** cells over their respective controls, after β-actin normalization. (**B and D**) Evaluation of protein expression by Western Blot analysis. *Upper panels*, histograms showing the relative optical density of TRF2 expression evaluated by Image-J quantification tool and normalized for β-actin. *Lower panel*, representative WB images of TRF2 and β-actin.
All the graphs show the mean (±SD) of at least three independent experiments (*$p< 0.1$, **$p< 0.01$, ***$p< 0.001$; Student's *t*-test).

Supplementary Figure S2

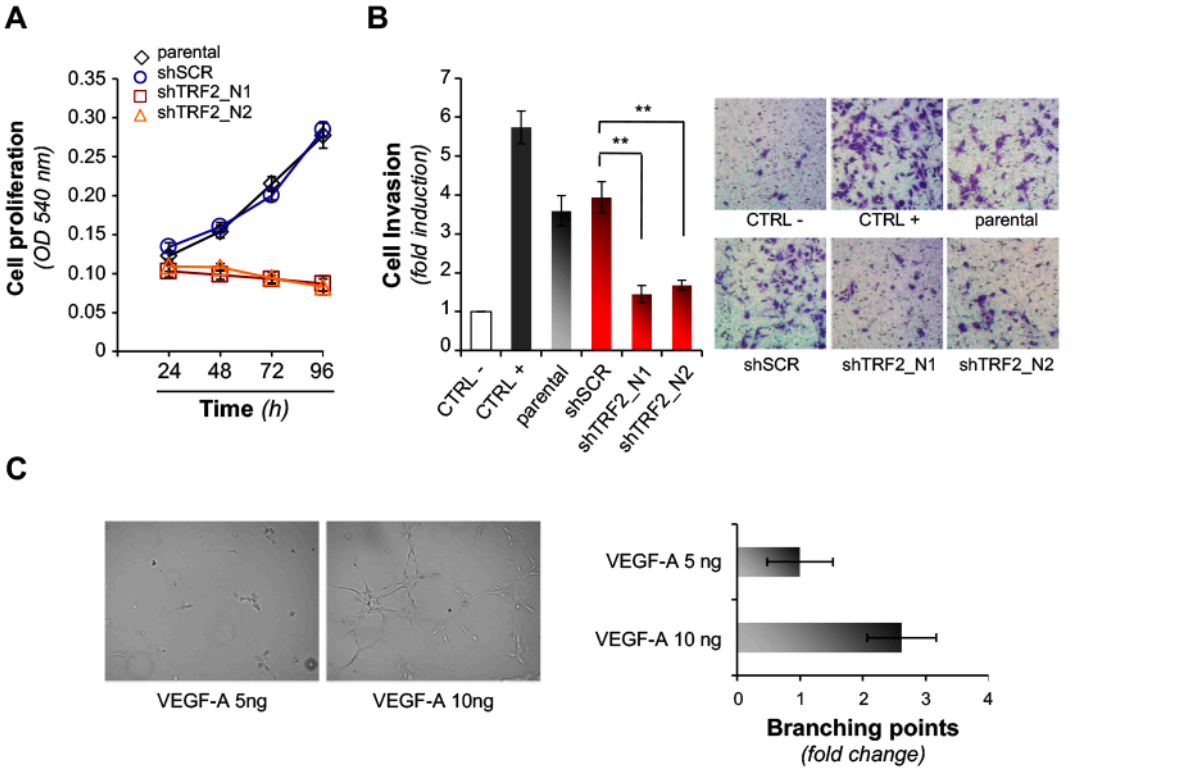

Supplementary Figure S2: TRF2 modulation affects the secretome of tumor cells and the angiogenic response of endothelial cells. (A) Proliferation of human umbilical vein endothelial cells (HUVEC) grown in the conditioned medium (CM) of HCT116 cells non infected (parental) or infected with lentiviral particles delivering short hairpin (sh) RNAs targeting TRF2 (shTRF2_N1 and shTRF2_N2) or a scramble sequences (shScramble). CMs were obtained from tumor cells grown under serum-deprivation for 48h. Proliferation was assessed by MTT colorimetric assay at the indicated times. **(B)** Invasion of HUVEC in response to CMs obtained as in A. Endothelial cell basal medium (EBM-2) and endothelial cell growth medium (EGM-2) were used as negative (CTRL-) and positive (CTRL+) controls, respectively. Histograms represent the mean number of invading cells. Results are expressed as fold change over negative control. For each sample, representative images are shown (5x magnification). **(C)** Tubule formation assay. HUVEC cells were seeded on Matrigel® in the presence of EBM-2 supplemented with an amount of VEGF-A (5 or 10 ng/well) corresponding at the concentration detected in the CM of shTRF2 and shScramble HCT116 cells, respecrively. Histograms show the mean number of branching points calculated on 5 different fields. *Left panel*: Representative images of tubular-like structures (5X magnification). *Right panel*: graphs show the mean ±SD of at least three independent experiments performed in triplicate. All the graphs show the mean ±SD of at least three independent experiments performed in triplicate (*p< 0.1, **p< 0.01, ***p< 0.001; Student's t-test).

Supplementary Figure S3

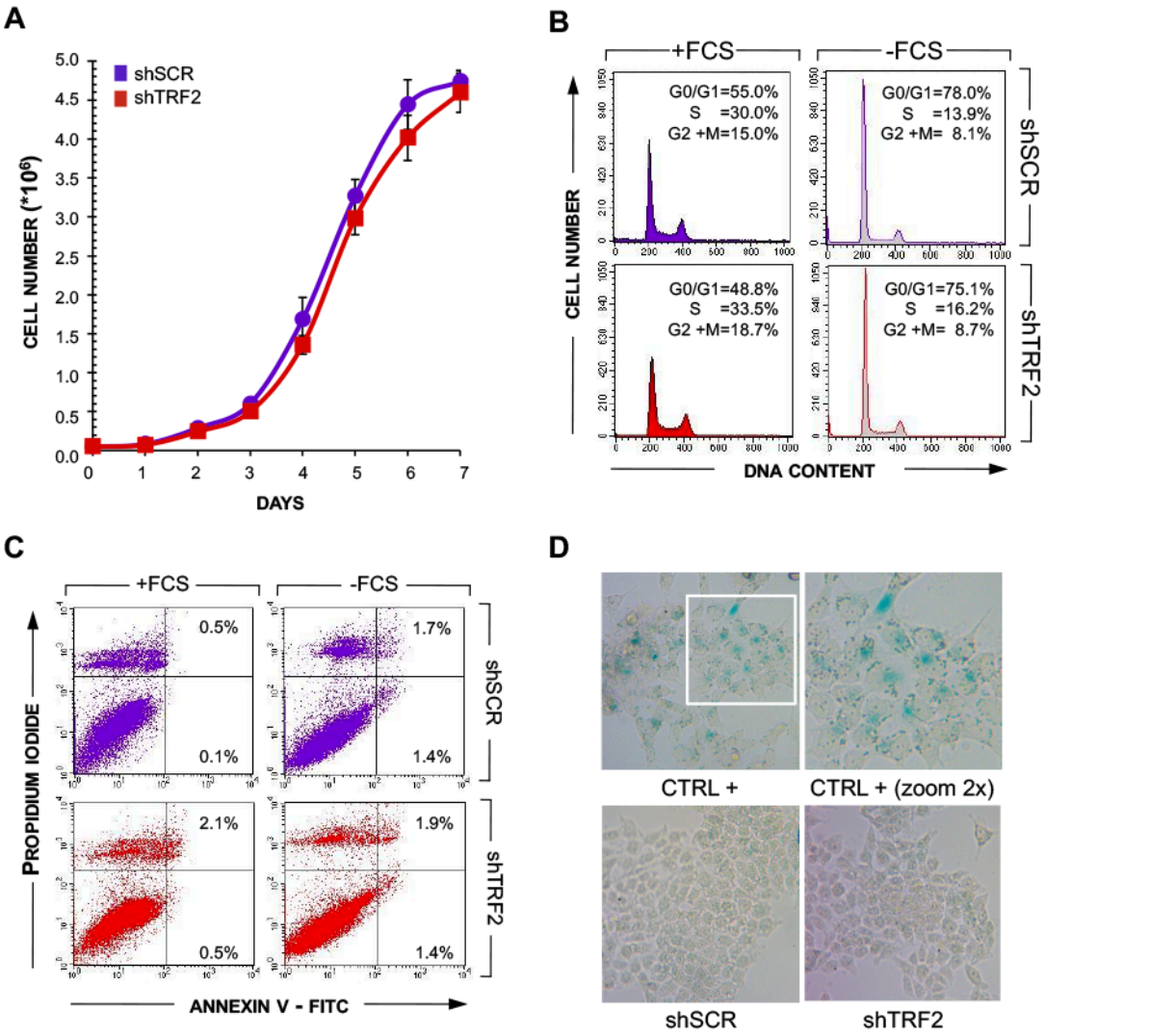

Supplementary Figure S3: TRF2 silencing in HCT116 does not affect cell growth and viability.
(A) HCT116 cells silenced for TRF2 (shTRF2) and their control counterpart (shScramble), were seeded ($5*10^4$ cells at day 0) and the proliferation was monitored through 7 day. **(B,C)** Cells from **A** were processed for FACS analysis to evaluate **(B)** cell cycle by PI staining and **(C)** apoptosis by annexin V expression. To evaluate the effect of serum, the experiments were also performed in cells maintained for 48h in serum-free medium before the analysis. **(D)** Cytochemical staining of senescence associated-βgal activity in HCT116 silenced (shTRF2) or not (shScramble) for TRF2. As positive control (CTRL +) parental HCT116 cells were treated with the G4 ligand RHPS4 (1 µM for 72h). Representative light microscopy images acquired at 10x magnification are shown.

Supplementary Figure S4

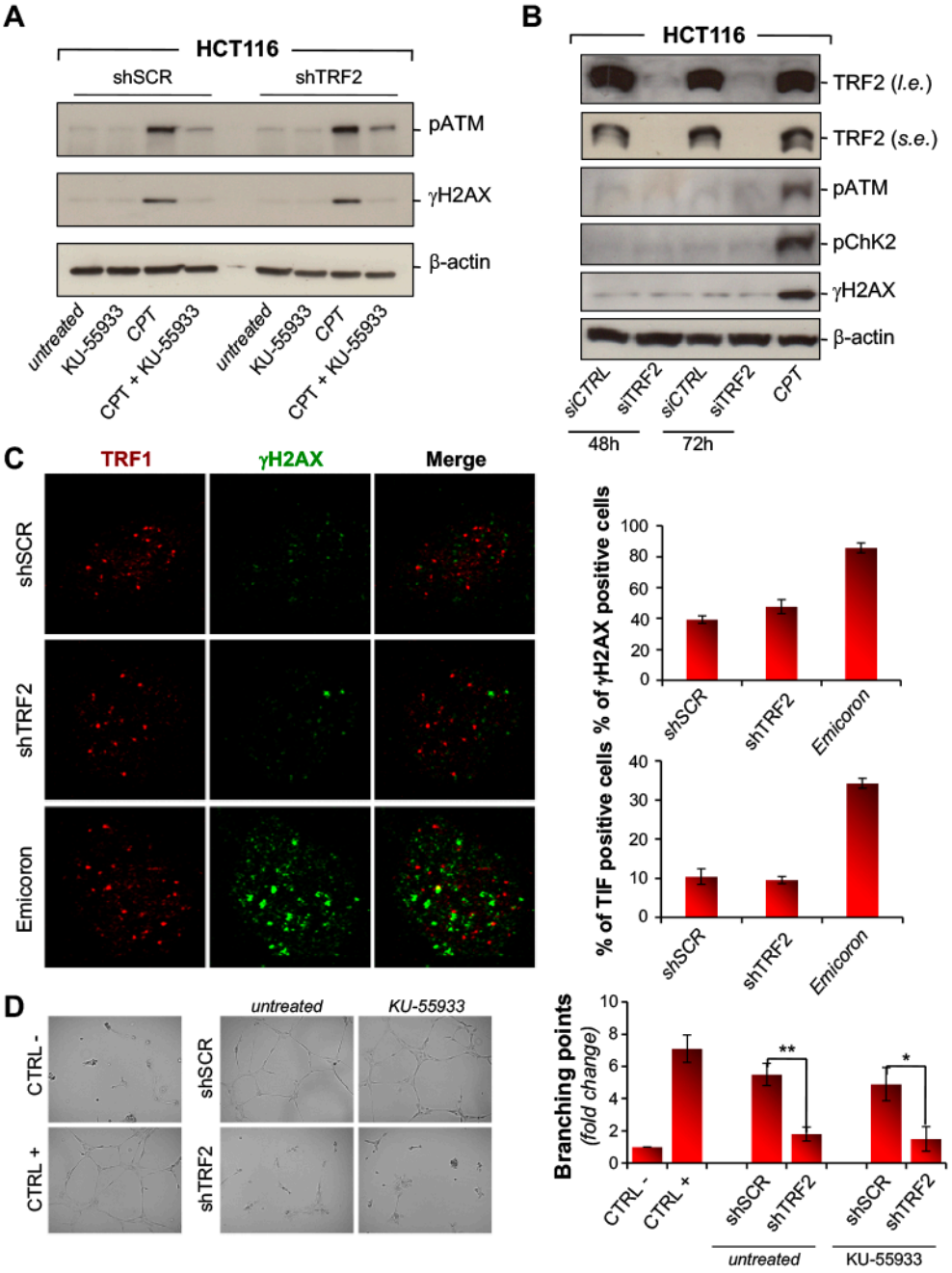

Supplementary Figure S4: TRF2 silencing in HCT116 does not induce DNA damage.
(A) Activation of DNA damage response (DDR) evaluated by Western Blotting in HCT116 cells knockdown for TRF2 (shTRF2) and their control counterpart (ShScramble, shSCR) serum starved for 48h. Analyses were performed in absence (untreated) or in presence of 5μM of the ATM-inhibitor KU-55933 (directly added in the serum-free medium for the last 24h). As an internal control, cells were treated with the DNA-damaging agent Camptothecin (CPT, 0.2 μM for 2h) in absence or in presence of KU-55933 (5μM, 24h). The picture shows WB images of phospho-ATM, phospho-H2AX (γ-H2AX) and β-actin. **(B)** HCT116 were transiently transfected with a siRNA against TRF2 (siTRF2) and the effect of silencing on the DDR pathway was evaluated by WB at the indicated times (48 and 72 h). Treatment with CPT (0.2 μM for 2h) was used as control. WB of TRF2 (long exposure, *l.e.* and short exposure, *s.e.*), phospho-ATM, phospho-ChK2, phospho-H2AX (γ-H2AX) and β-actin are shown. **(C)** Immunofluorescence analysis of telomere damage. *Left panel*, representative images of confocal sections used in the detection of TRF1 (red) and γH2AX (green) co-localization at telomere damage-induced foci (TIF) in cell silenced (shTRF2) or not (shSCR) for TRF2. Treatment with the G4 ligand Emicoron (1 μM for 24 h) was used as positive control (CTRL +). *Right panel*, quantification of γH2AX (upper histogram) and TIF (lower histogram) positive cells, as estimated by scoring the spots counted in all of the confocal sections of a nucleus. **(D)** CM obtained from the cells described in **A** were assayed for their capability of inducing tubular-like structure in HUVEC cells seeded on Matrigel®. EBM-2 and EBM-2 supplemented with VEGF-A (100 ng/ml) were used as negative and positive controls, respectively. *Left panel*, representative microscopy images showing tubular-like structures (5x magnification). *Right panel*, hisograms showing the mean number of branching points calculated on 5 different fields and expressed as fold induction over the negative control. All the graphs show the mean ±SD of at least three independent experiments (*$p< 0.1$; **$p< 0.01$; ***$p< 0.001$; Student's *t*-test).

Supplementary Figure S5

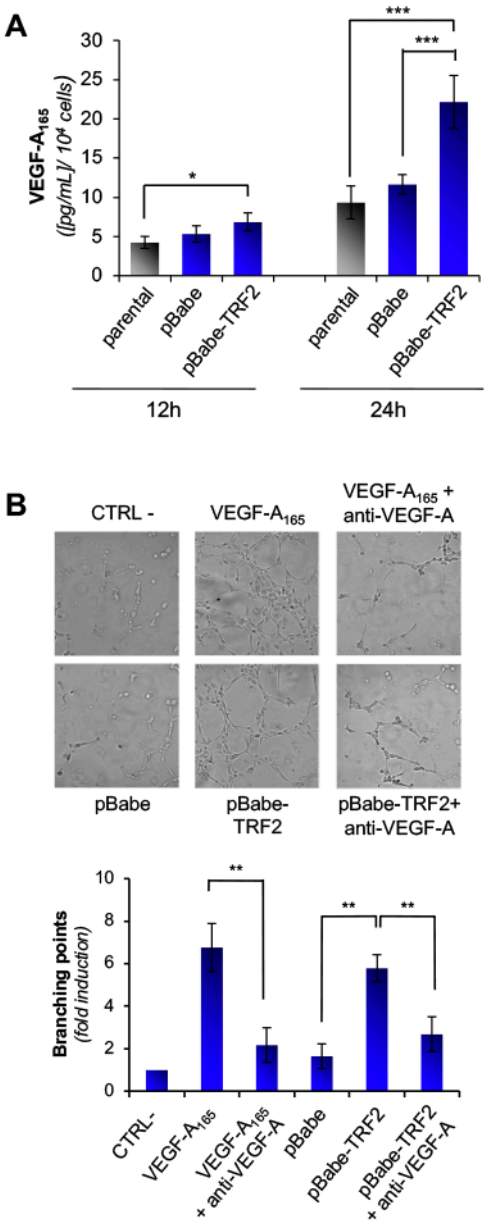

Supplementary Figure S5: TRF2 affects tumor angiogenesis by inducing a time-dependent release of VEGF-A in the CM of tumor cells. (A) Concentration of VEGF-A was evaluated by ELISA in the CM of HCT116 overexpressing TRF2 (pBabe-TRF2), collected 12 h and 24 h after serum-starvation. As control, the amount of VEGF-A was assayed in the CM of HCT116 cells not infected (parental) or infected with viral particles delivering control vectors (pBabe). Results were normalized to cell number. Histograms show the mean (±SD) of at least three independent experiments performed in triplicate (*p< 0.1, ***p< 0.001; Student's t-test). **(B)** CM obtained from HCT116 cells overexpressing TRF2 (pBabe-TRF2) growth for 24 h in serum-free medium was incubated in absence or in presence of an anti-VEGF-A165 blocking antibody (1 mg/ml for 30 minutes) and assayed for the capability of inducing HUVEC differentiation. CM from HCT116 transduced with the empty vector was used as an internal control while EBM-2 supplemented or not with VEGF-A (100 ng/ml) was used as positive and negative control, respectively. The effectiveness of the antibody was assessed on the positive control. Histograms show the mean number of branching points calculated on 5 different fields and expressed as fold induction over the negative control. Upper panel: pictures show representative images of tubular-like structures (5x magnification). Lower panel: histograms show the mean (±SD) of at least three independent experiments (*p< 0.1, **p< 0.01, ***p< 0.001; Student's t-test).

Supplementary Figure S6

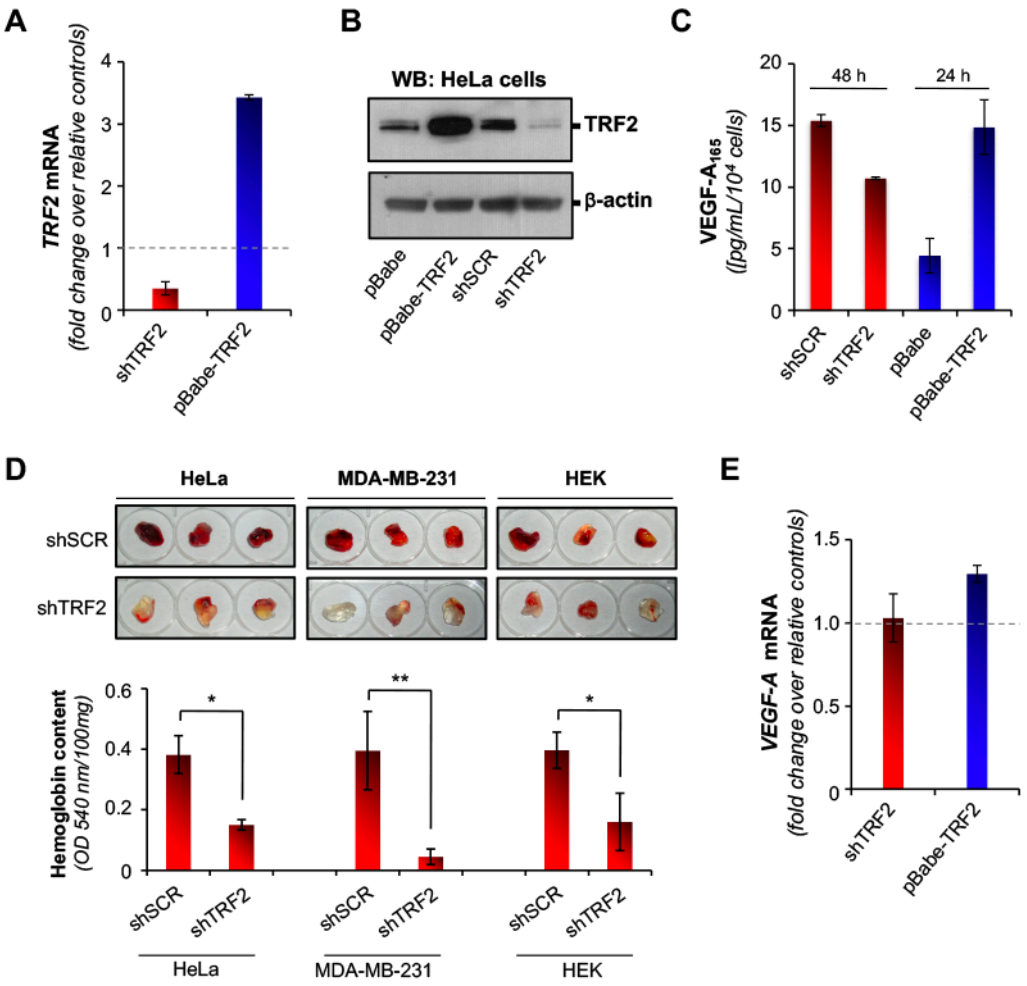

Supplementary Figure S6: TRF2 controls angiogenesis by regulating the VEGF-A levels in the secretome of various tumor cells.
(A and B) Levels of TRF2 expression were evaluated in stable HeLa cells silenced (shTRF2) or overexpressing (pBabe-TRF2) TRF2 and in their control counterparts (shScramble/ pBabe). **(A)** Quantitative evaluation of gene expression by *real-time* RT-PCR. Results are expressed as fold change of mRNA levels in silenced/overexpressing cells over their respective controls, after β-actin normalization. (**B**) Evaluation of protein expression. The picture shows a representative WB image of TRF2 and β-actin. **(C)** Concentration of VEGF-A was evaluated by ELISA in the CM derived from TRF2-compromised (shTRF2) or -overexpressing (pBabe-TRF2) HeLa cells and their control counterparts (shScramble/pBabe). CMs were collected 48 h after the serum-starvation for silencing experiments, and at 24 h for overexpression experiments. **(D)** CMs from HeLa (*left*), MDA-MB-231 (*middle*) or HEK (*right*) cells silenced (shTRF2) or not (shScramble, shSCR) for TRF2, collected after 48 h of serum-deprivation, were assayed for their angiogenic potential *in vivo*. *Upper panel*, pictures showing the Matrigel® plugs recovered 5 days post-injection. *Lower panel*, histograms representing the average hemoglobin content measured in the relative samples and expressed as absorbance (OD_{540nm})/ mg of Matrigel® (n = 8 plugs per group; *p< 0.1, **p< 0.01, ***p< 0.001; Student's t-test) **(E)** Quantification by *real-time* RT-PCR of VEGF-A gene expression in stable HeLa cells from **a**. Histogram shows the fold change of mRNA in silenced/overexpressing cells over their respective controls, after β-actin normalization.

Supplementary Figure S7

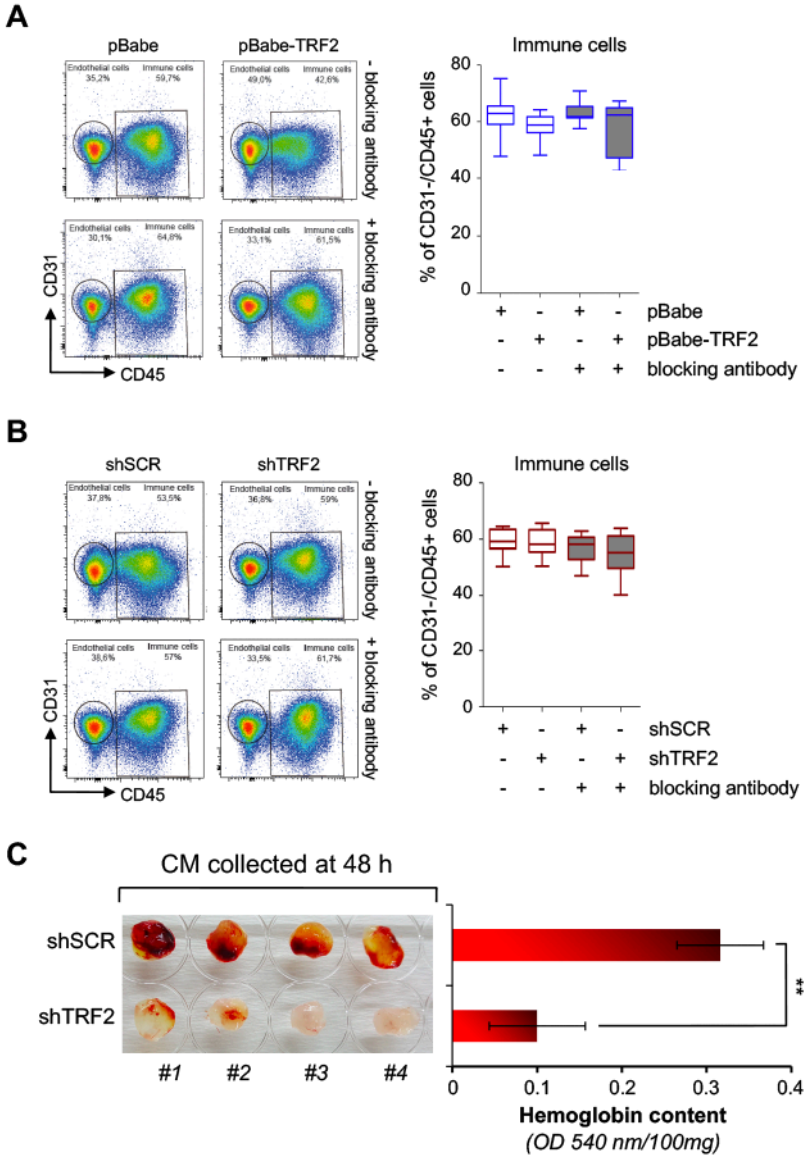

Supplementary Figure S7: Immune cells do not contribute to modulation on angiogenic response *in vivo*.
(A and B) Evaluation of immune cell recruitment induced by CMs derived from HCT116 cells **(A)** overexpressing (pBabe-TRF2) or **(B)** silenced for TRF2, collected after serum starvation for 24 and 48 h, respectively. For each experiment the CMs from control cells (pBabe or shScramble) were also assayed. Where indicated the analyses were performed in presence of the blocking antibody against VEGF-A (1 µg/ml for 30 min). The indicated CMs, premixed with Matrigel®, were injected subcutaneously into C57BL/6 mice and the immune infiltrate in the Matrigel® plugs was examined by FACS analysis. *Left panels*, FACS analysis show the percentage of endothelial (CD31-/CD45- cells) and immune cells (CD31-/CD45+ cells). *Right panels*, minimum to maximum box-and-whiskers graphs showing the percentage of recruited immune cells. **(C)** CMs from HCT116 cells interfered (shTRF2) or not (shScramble) for TRF2 were assayed for their angiogenic potential in immune-depleted NSG mice *in vivo*. *Left panel*, picture shows Matrigel® plugs recovered 5 days post-injection. *Right panel*, histogram represents the average hemoglobin content measured in the relative samples and expressed as absorbance (OD_{540nm})/ mg of Matrigel® (n = 8 plugs per group; *p< 0.1, **p< 0.01, ***p< 0.001; Student's t-test).

Supplementary Figure S8

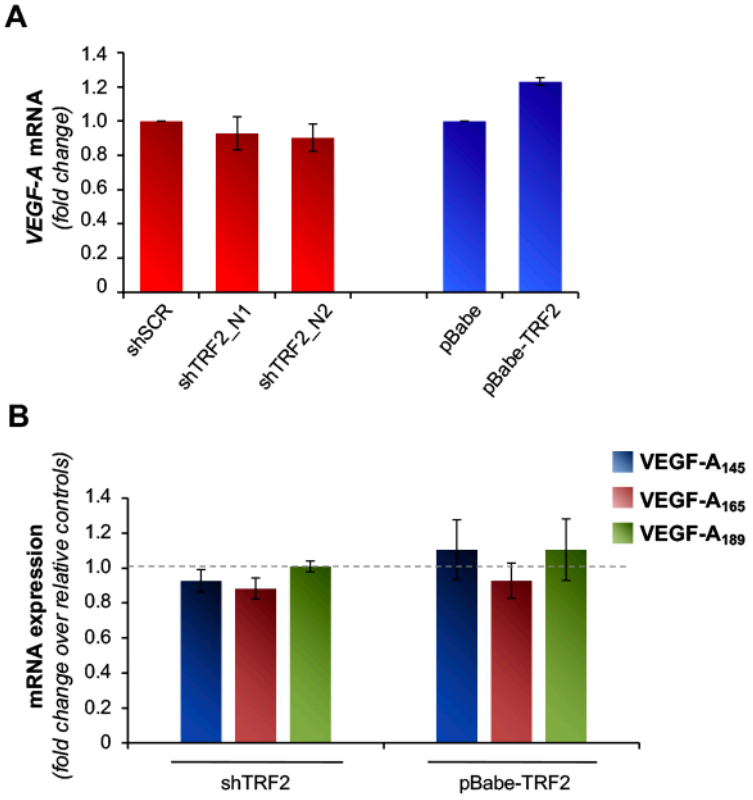

Supplementary Figure S8: TRF2 does not affect the gene expression of VEGF-A.
Transcription levels of VEGF-A were quantified in HCT116 stably silenced (shTRF2_N1 and shTRF2_N2) or overexpressing (pBabe-TRF2) TRF2 and in their control counterparts (shScramble and pBabe). R*eal-time* RT-PCR analysis performed with **(A)** primers that recognize the overall mRNA of VEGF-A or **(B)** specific primers for VEGF-A_{145}, VEGF-A_{165}, VEGF-A_{189} isoforms. Histograms show the fold change of mRNA in silenced/overexpressing cells over their respective controls, after β-actin normalization. All the graphs show the mean ±SD of at least three independent experiments performed in triplicate.

Supplementary Figure S9

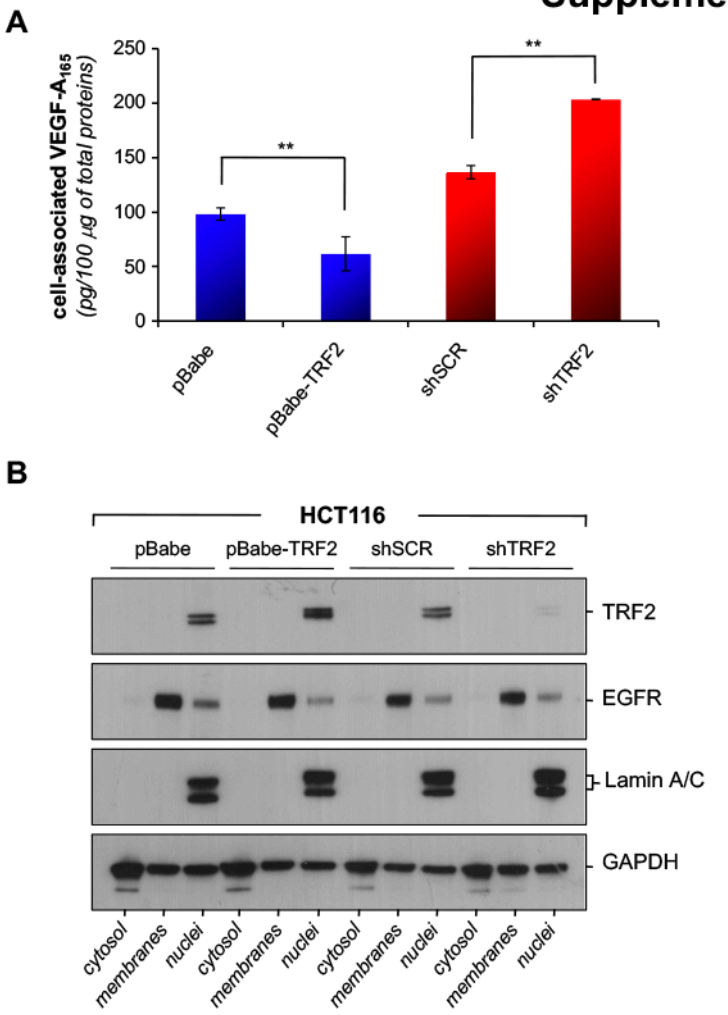

Supplementary Figure S9: TRF2 modulation affects the cellular levels of VEGF-A.
(A) Amount of cell-associated VEGF-A_{165} was quantified by ELISA. Analyses were performed on cell lysates obtained from HCT116 cells silenced (shTRF2) or overexpressing (pBabe-TRF2) TRF2 and their controls (shScramble and pBabe). Results were normalized to the total amount of proteins. Histogram shows the mean ±SD of three independent experiments performed in triplicate (*$p< 0.1$, **$p< 0.01$, ***$p< 0.001$; Student's *t*-test). **(B)** Cell lysates from **a** were divided into subcellular fractions (cytosol, membrane, and nuclear extracts). Representative western blot images showing the distribution of EGFR, Lamin A/C and GAPDH in the different cell fractions. TRF2 expression levels were evaluated as control.

Supplementary Figure S10

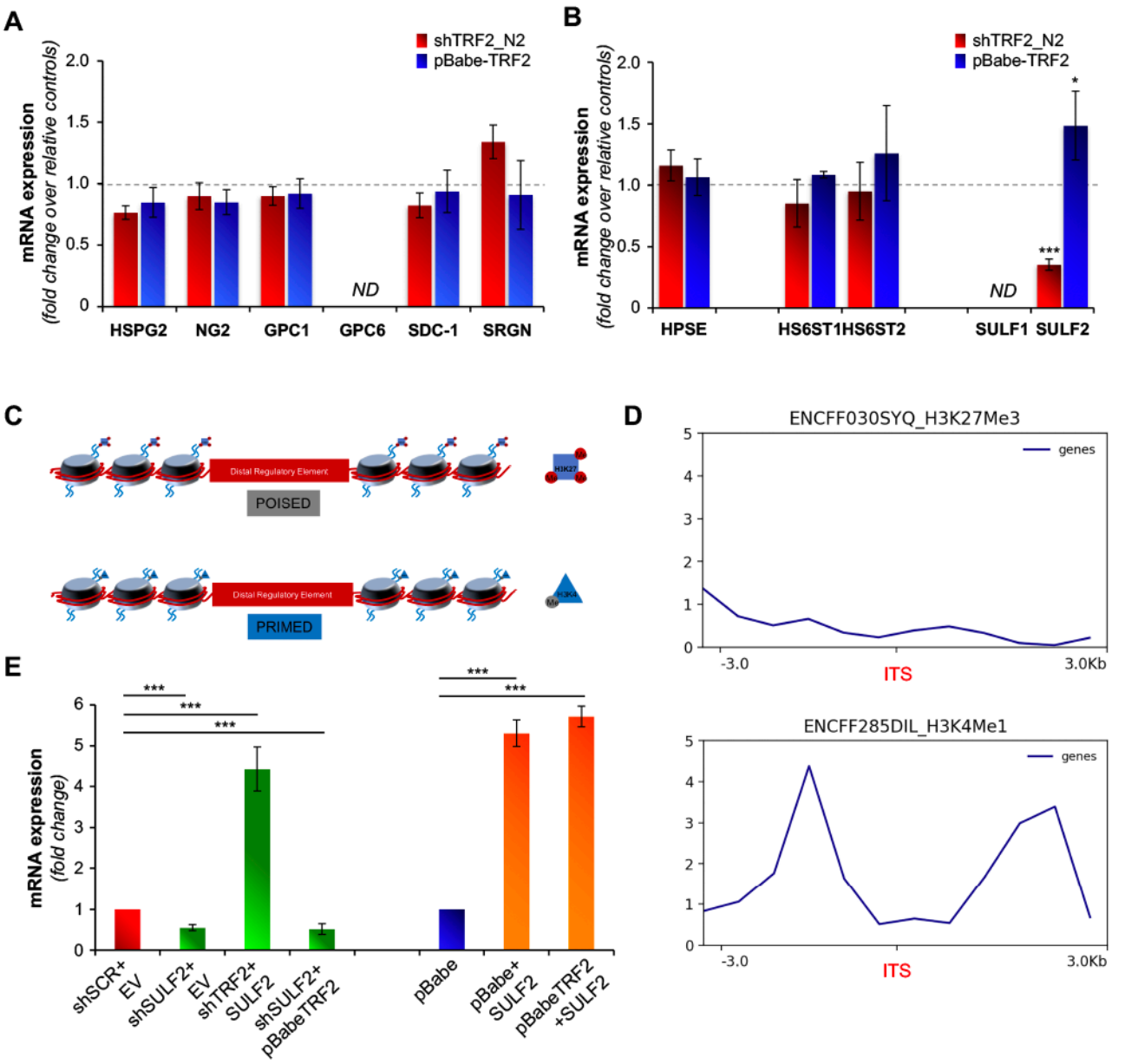

Supplementary Figure S10: TRF2 affects SULF2 expression through the binding to a distal regulatory element.
(A and B) HCT116 cells silenced (shTRF2) or overexpressing (pbabe-TRF2) TRF2 and their control counterparts (shSCR and pBabe) were evaluated by R*eal-time* RT-PCR for the expression levels of the genes encoding for the indicated **(A)** membrane HSPGs and **(B)** HSPG-modifying enzymes. Histograms show the fold change of mRNA in silenced/overexpressing cells over their respective controls, after β-actin normalization. **(C)** Schematic representation resuming the features of distal regulatory elements and their associated chromatin modification states. **(D)** Histograms showing H3K27me3 (upper panel) and H3K4me1 (lower panel) peaks on the 6 kilobases (Kb) region around the identified ITS (ENCODE data for the HCT116 cells). **(E)** R*eal-time* RT-PCR analysis of SULF2 silencing or overexpression in HCT116 cells. Results show the fold change of mRNA in cells silenced/overexpressing SULF2 respect to their controls. Histograms show the mean ±SD of at least three independent experiments performed in triplicate (*$p< 0.1$, **$p< 0.01$, ***$p< 0.001$; Student's *t*-test).

Supplementary Figure S11

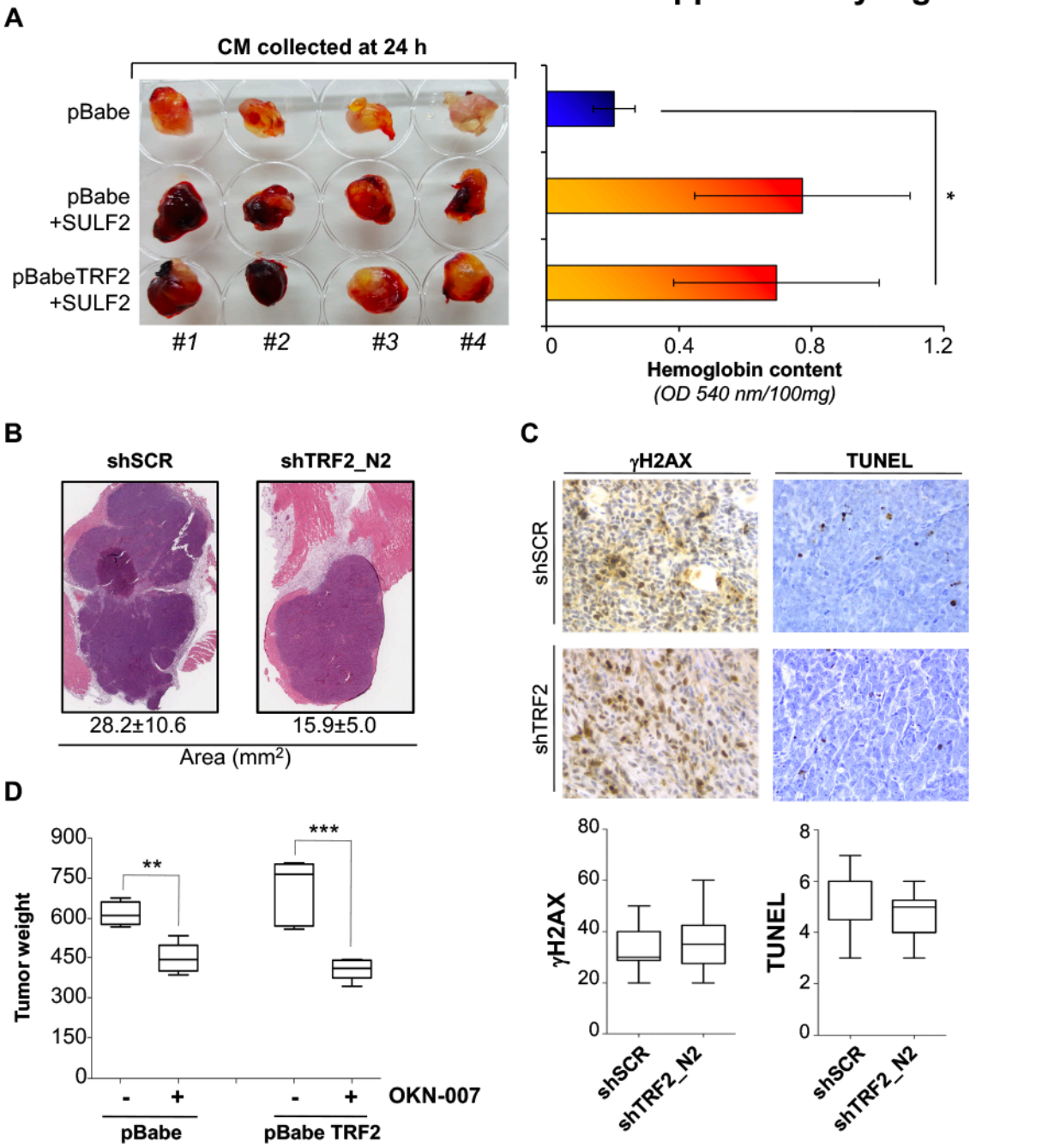

Supplementary Figure S11: Effects of TRF2 modulation on HSPGs.
(A) Angiogenic potential of CMs obtained from HCT116 cells overexpressing *TRF2* (pBabe-TRF2) and their control counterpart (pBabe), infected or not with lentiviral particles delivering the construct encoding for *SULF2* was evaluated *in vivo* by Matrigel® assays. *Left panel:* representative pictures showing the Matrigel® plugs recovered 5 days post-injection. *Right panel:* histogram representing the average hemoglobin content measured in the relative samples and expressed as absorbance (OD540nm)/ mg of Matrigel® (n = 8 plugs per group; *p< 0.1, **p< 0.01, ***p< 0.001; Student's t-test). **(B)** HCT116 cells silenced for TRF2 (shTRF2_N2) and their control counterpart (shScramble, shSCR) were inoculated intramuscularly in immunocompromised mice and tumor area of two tumors stained with H&E was evaluated at day 14 after cell injection. Representative images of tumors are shown. Data are mean ± SD from 2 mice per group. **(C)** IHC analyses of the tumors from B. *Upper panel:* representative IHC images of γH2AX and TUNEL staining. *Lower panel*: quantitative analysis of the indicated markers. Data are mean (±SD) from 2 mice per group (*p< 0.1, **p< 0.01, ***p< 0.001; Mann–Whitney test). **(D)** HCT116 cells overexpressing TRF2 (pBabe TRF2) and their control counterpart (pBabe) were intramuscularly injected in nude mice untreated or treated with the SULF2 inhibitor OKN-007 (50 mg/kg once a day for two weeks) and the tumor weight was evaluated 34 days after cell injection. The graph shows the mean ±SD from 5 mice per group (*p< 0.1, **p< 0.01, ***p< 0.001; Student's t-test).

Supplementary Table S1. Primer sequences used for real-time PCR experiments.

Gene	Primer FWD	Primer REV
ACTIN	AGCACTGTGTTGGCGTACAG	TCCCTGGAGAAGAGCTACGA
VEGF-A	GAGCCTTGCCTTGCTGCTCTAC	CACCAGGGTCTCGATTGGATG
TERF2	CTGAGCTCACACCACTGGAA	GCATCTTCTGCTGGAAGGTC
$VEGF\text{-}A_{145}$	ATCTTCAAGCCATCCTGTGTGC	TCGGCTTGTCACATACGCTCC
$VEGF\text{-}A_{165}$	ATCTTCAAGCCATCCTGTGTGC	CAAGGCCCACAGGGATTTTC
$VEGF\text{-}A_{189}$	ATCTTCAAGCCATCCTGTGTGC	CACAGGGAACGCTCCAGGAC
SULF2	GGC AGG TTT CAG AGG GAC C	GAAGGCGTTGATGAAGTGCG
SULF1	ATGCAGGTTCTTCAAGGCAG	ATCCTGGTTGAATAATCAATCTCT
HSPG2	TCGGCCATGAGTCCTTCTAC	CCTGCTGTGTAGGAGAGGGT
SDC-1	CTCTGGCTCTGGCTGTGC	AGCCATCTTGATCTTCAGGG
GPC-1	AGATCTACGGAGCCAAGGG	TGTAGCCCTGGGGACAGAT
GPC-6	TGGAAGACAAGTTAAGCCAACAA	TTCTTATGCCTGGACACAAAAGT
SRNG	TCCTGGTTCTGGAATCCTCA	TTCTTCAAGGCAGTTTGCAG
HPSE	TGGCAAGAAGGTCTGGTTAGGAGA	GCAAAGGTGTCGGATAGCAAGGG
NG2	TATGTTGGCCAGACTTGCAT	TGCAGGTCTATGTCGGTCAG
HS6ST1	CGACTGGACCGAGCTCAC	GGTCTCGTAGCAGGGTGATG
HS6ST2	TGCTCCCAGAATCATCAGCC	GGGCATTTTCTGGAAGGCGA

Supplementary Table S2. Primer sequences used for ChIP assay.

Target region	Primer FWD	Primer REV
RPLP0	GCGCCCATCTAACTAGCACA	TCGCGACCCTACTTAAAGGC
Chr.2 (sub-telomeric region)	CCCAAACCCTAACCCTAAAA	CTTCCTGTTTGCAGCACTGA
SULF2 (region 1)	GTGATCCACCCATCTTGGTC	CATGCCAATCCAGAAACTCA
SULF2 (region 2)	ACAGCCCCAGAAGAAGGGAT	TTCCTGAACATGGCTCTCCC

Supplementary Table S3. Nucleotide sequence of the genomic region cloned in the PGL3 vector.

```
  1 caagtgttgg gtttacaggc atgagcgacc atgcctggcc cccactttct cttcttagaa
 61 ggataccaat cattggatta gggtccaccc taatctaagt attacaccct catcttaact
121 atctgcagct gcaaggtccc caattccaca taaggtcaca ttctgagttt ctggattggc
181 atgaattggg g
```

Supplementary Table S4. Bio-pathological characteristics of colorectal carcinomas

Total number of pts	169
Tumor size	
1-2	16 (9.4%)
3	112 (66.3%)
4	41 (24.3%)
Node	
Negative	79 (47%)
Positive	90 (53%)
Grading	
1-2	139 (82%)
3	30 (18%)
Stage	
I-II	67 (40%)
III	61 (36%)
IV	41 (24%)
TRF2 expression	
0	30 (17.7%)
1+	26 (15.4%)
2+	65 (38.5%)
3+	48 (28.4%)
SULF2 expression	
IRS* ≤ 15	61 (36.1%)
IRS > 15	108 (63.9%)
* (staining intensity x percentage of positive cells)	